# Nature of the photonic band gap: some insights from a field analysis

R. D. Meade, A. M. Rappe, K. D. Brommer, and J. D. Joannopoulos

*Department of Physics, Massachusetts Institute of Technology, Cambridge, Massachusetts 02139*

Received May 15, 1992; revised manuscript received September 4, 1992

To clarify the nature of photonic band gaps, a series of calculations on two-dimensional photonic crystals is undertaken. Systems that possess a large gap for one polarization and no gap for the other polarization are analyzed. Two features of a photonic crystal that give rise to a large photonic band gap for each polarization, i.e., connectivity and concentration of the dielectric material, are elucidated. The implications for making materials with large photonic band gaps in two and three dimensions are discussed.

## INTRODUCTION

In recent years several dielectric structures were found to possess a photonic band gap,[1,2] a range of frequencies for which no propagating states exist. The existence of a photonic band gap gives rise to a number of interesting and useful properties, including the localization of light at defects[3,4] and at surfaces[5,6] and the inhibition of radiation.[7,8] These properties become more pronounced as the photonic band gap is made larger. Therefore, to permit us to take maximal advantage of the ability of photonic crystals to control electromagnetic radiation, development of photonic crystals with large band gaps is important.

The search for crystals with large band gaps has been extensive.[1,2,9–13] For three-dimensional systems considerable experimental and computational effort has been expended in testing various configurations of dielectrics to see which ones would yield the largest gap. This trial-and-error search has identified structures with significant band gaps (gap/midgap ratio of ~20%). However, this method does not address the question of why a particular structure has a large band gap.

In this paper we attempt to elucidate why some photonic crystals have gaps and others do not. Ideally we would like to generate some simple and intuitive rules that determine the presence and the size of gaps. For a number of reasons this is a difficult undertaking. The photonic crystals that contain gaps often have a complex dielectric structure, there is always the possibility of band gaps between high-frequency bands or at high dielectric contrast, and in general it is difficult to get an intuitive grasp of the solutions to Maxwell's equations at different special points in complex dielectric structures. For these reasons we have chosen to study the presence of gaps in two-dimensional structures (as in Refs. 10 and 12–14) with the hope that the knowledge gained from this simpler case may provide insight into the nature of photonic band gaps in complex three-dimensional structures. For simplicity we consider only the gap between the first and the second bands, which we call the dielectric and the air bands, and we consider only moderate index contrasts (3:1).

One reason that these two-dimensional systems are easier to analyze is that the eigenmodes must be either TE, with fields along $(H_z, E_x, E_y)$, or TM, with fields along $(E_z, H_x, H_y)$, where the two-dimensional photonic crystal is oriented along the $z$ direction. Because these modes separate, we can identify the reasons for the presence of band gaps in each polarization independently. Moreover, because the $E$ field must be either in the plane $(E_x, E_y)$ or normal to it $(E_z)$, it is simpler to visualize the modes of these two-dimensional systems than those of their three-dimensional counterparts.

With this motivation we proceed as follows. After describing how these computations were performed, we examine the band structure of square arrays of dielectric cylinders and of square holes, as shown in the insets to Figs. 1 and 2 below. These two systems are complementary in the sense that one is connected and the other is not and that one has all its dielectric material concentrated about one point in the unit cell and the other does not. We shall see that the dielectric lattice of dielectric cylinders has a large gap for TM modes but none for TE modes. On the other hand, the reverse is true for the array of square holes, which has a large gap for TE modes but none for TM modes. We explain this difference in band structure based on the qualitative differences in the lattice. To do so, we examine the field patterns of these two lattices at the Brillouin-zone edge as well as by considering the modes' fill factors, the amount of electromagnetic energy localized in the dielectric regions.

## ANALYSIS

To analyze the electromagnetic behavior of photonic crystals, we solve Maxwell's equations in macroscopic media by expanding the electromagnetic eigenstates in plane waves.[1] Briefly, a single governing equation for electromagnetic states can be found by rearranging Maxwell's equations in macroscopic media:

$$\nabla \times \left( \frac{1}{\epsilon(\mathbf{r})} \nabla \times \mathbf{H} \right) = \frac{\omega^2}{c^2} \mathbf{H}. \tag{1}$$

Here $\epsilon(\mathbf{r})$ is the dielectric function and $\mathbf{H}$ is the magnetic field of an electromagnetic mode of frequency $\omega$. The magnetic field, which must be transverse ($\nabla \cdot \mathbf{H} = 0$), is

0740-3224/93/020328-05$05.00 

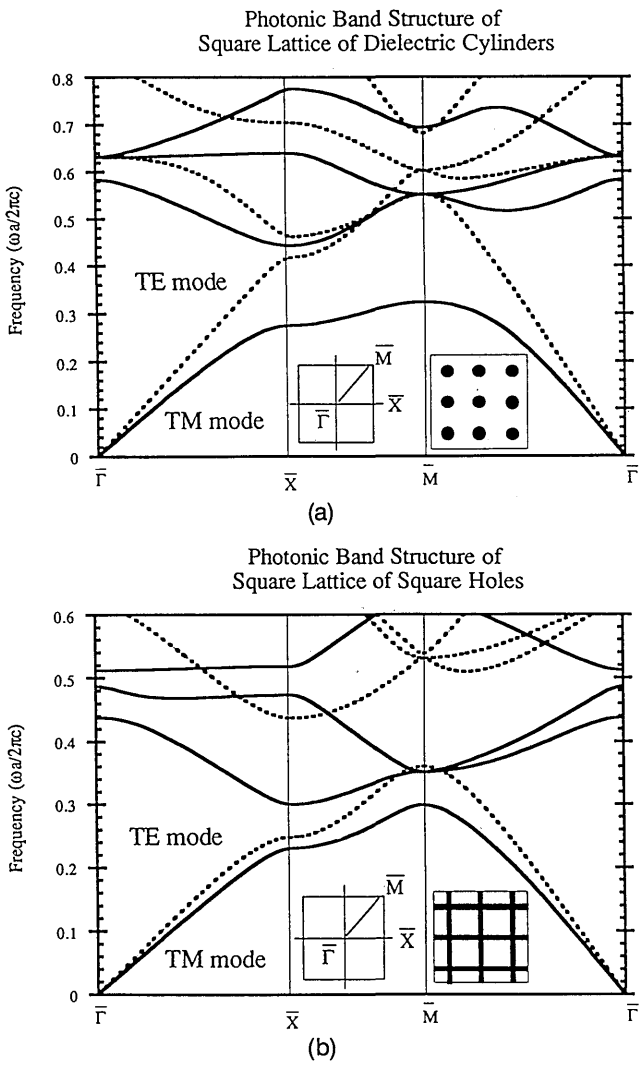


Fig. 1. Photonic band structures, showing the relationship between frequency and wave vector for the lowest-frequency propagating electromagnetic modes. Solid curves represent TM modes, with fields along $(E_z, H_x, H_y)$, and dashed curves represent TE modes, with fields along $(H_z, E_x, E_y)$. The left-hand inset of each figure shows the high-symmetry points within the two-dimensional Brillouin zone. The right-hand insets show a cross-sectional view of the dielectric function, with the shaded area representing high dielectric constant. (a) Modes inside a square array of high-dielectric ($\epsilon = 8.9$) cylinders. (b) Modes inside a square array of square holes in a high-dielectric material.

then expanded in a basis of transverse plane waves, $\mathbf{e}_\lambda \exp[i(\mathbf{k} + \mathbf{G}) \cdot \mathbf{r}]$, where $\mathbf{e}_\lambda$ are the unit vectors perpendicular to wave vector $\mathbf{k} + \mathbf{G}$. In this basis Eq. (1) becomes a matrix eigenvalue equation,

$$\sum_{(\mathbf{G}\lambda)'} \Theta^{\mathbf{k}}_{(\mathbf{G}\lambda),(\mathbf{G}\lambda)'} h_{(\mathbf{G}\lambda)'} = \omega^2 h_{(\mathbf{G}\lambda)}, \tag{2}$$

where $h_{\mathbf{G}\lambda}$ is the coefficient of the plane wave $\mathbf{e}_\lambda \exp[i(\mathbf{k} + \mathbf{G}) \cdot \mathbf{r}]$ and the matrix $\Theta$ is defined by

$$\Theta^{\mathbf{k}}_{(\mathbf{G}\lambda),(\mathbf{G}\lambda)'} = [(\mathbf{k} + \mathbf{G}) \times \mathbf{e}_\lambda] \cdot [(\mathbf{k} + \mathbf{G}') \times \mathbf{e}_{\lambda'}] \epsilon^{-1}(\mathbf{G}, \mathbf{G}'). \tag{3}$$

In this expression $\epsilon^{-1}(\mathbf{G},\mathbf{G}')$ is the inverse of the Fourier transform of the dielectric function $\epsilon(\mathbf{r})$. This eigenvalue equation can now be solved by standard numerical techniques, yielding the normal mode coefficients and frequencies of the electromagnetic modes. Because of the two-dimensional nature of the problems considered, convergence was achieved with a relatively small number of plane waves. We estimate that with the 1600 plane waves per polarization the electromagnetic mode frequencies were calculated to an accuracy of better than 1%. This technique provides a simple way to solve problems in electrodynamics that takes full account of the vector nature of electromagnetic radiation.

The band structures are calculated for two dielectric lattices. The first structure is created by orienting an array of cylinders of high dielectric strength ($\epsilon = 8.9$, the dielectric constant of alumina) in a square lattice. A cross section of this crystal is shown as an inset to Fig. 1(a). The radius of the cylinders is chosen to be $0.2a$, where $a$ is the crystal lattice constant. This structure corresponds to the experimental setup of Robertson *et al.*[14] The second structure is created by beginning with a high-dielectric ($\epsilon = 8.9$) material and removing a square array of square holes from it. A cross-sectional view of this structure is shown as an inset to Fig. 1(b). The square holes were chosen to have length $0.84a$ on a side.

The photonic band structures for the two dielectric arrays are shown in Fig. 1. Clearly the lattice of dielectric cylinders has a complete gap for TM modes (solid curves) but not for TE modes (dashed curves). The reverse is true for the array of square holes, which has a gap for TE modes but not for TM modes. It is important to note that all these structures still exhibit small splittings between all bands at the $X$ point and most bands at the $M$ point. This is a consequence of band repulsion, which is well known in electronic band structures. Because all these bands exhibit some splitting, our goal in this investigation is to discover why some splittings are large and others are small.

To investigate the size of the splitting, we examine the field patterns of states for each polarization of each structure, shown in Figs. 2–5. Each of these figures shows the displacement field, $\mathbf{D}(\mathbf{r})$. For the TM modes this displacement field is oriented normal to the plane, $\mathbf{D}(\mathbf{r}) = d(\mathbf{r})\hat{z}$, where $d(\mathbf{r})$ is a real scalar function. In Figs. 2 and 4 the height of the surface represents $d(\mathbf{r})$, the size of the $z$ component of $\mathbf{D}(\mathbf{r})$. For the TE modes this displacement field is oriented in the plane, $\mathbf{D}(\mathbf{r}) \cdot \hat{z} = 0$. In Figs. 3 and 5 the displacement field is represented by field lines. In all cases the fields are shown at the $M$ point, $\mathbf{k} = (G/2, 0)$. The fields at those zone-edge states have opposite phases in each unit cell in the direction of the wave vector ($x$) and constant phases in each unit cell perpendicular to the wave vector.

### TM Modes in Dielectric-Rod Array

The TM modes of this structure have a large gap. In Fig. 2(a) we see that the fields associated with the dielectric material are strongly concentrated in the dielectric regions. This contrasts strongly with Fig. 2(b), which shows the field pattern of the air band. Here a nodal plane cuts through all the dielectric cylinders, expelling some of the displacement field amplitude from the dielectric region.

Clearly the frequency of light for a given wavelength is lower in dielectric material than in air. It seems reason-

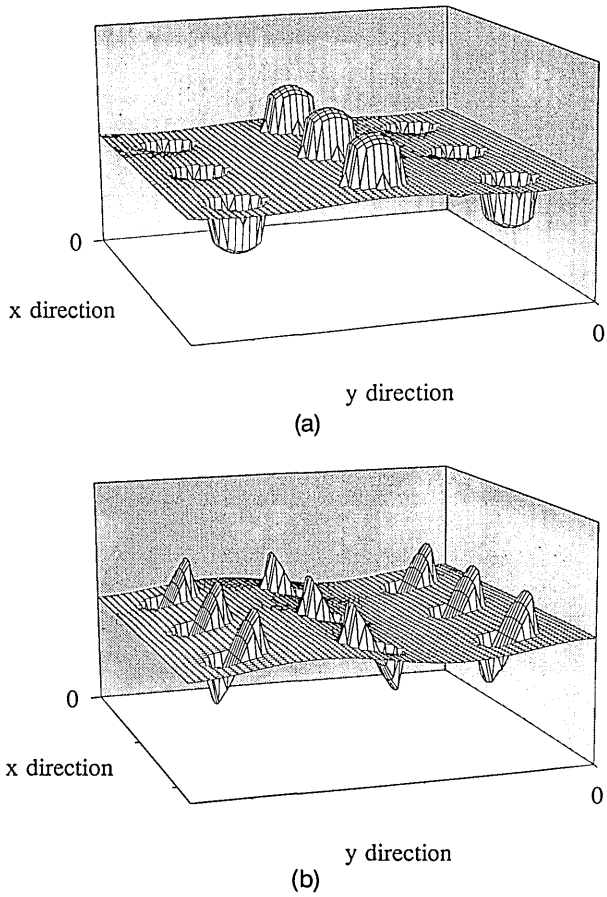


Fig. 2. Displacement fields of $X$-point TM states inside a square array of high-dielectric ($\epsilon = 8.9$) cylinders. TM modes have $\mathbf{D}$ normal to the plane, $\mathbf{D}(\mathbf{r}) = d(\mathbf{r})\hat{z}$. The height of the surface represents the size of the $z$ component of the displacement field. Positive peaks represent displacement fields pointing up the cylinders, and negative peaks show displacement fields pointing down the cylinders. (a) Dielectric-band state; (b) air-band state.

able, then, that eigenmodes that have most of their character in the dielectric region have lower frequency than those with most of their energy in air. This simple observation explains the large splitting between these two bands: the first band has most of its character in the dielectric regions and has a low frequency, while the second has most of its character in the air and a higher frequency. This behavior is corroborated by comparing the fill factor for these two bands, defined as

$$f = \frac{\int_{V_{\epsilon=8.9}} \mathbf{E}^*(\mathbf{r}) \cdot \mathbf{D}(\mathbf{r}) d^3\mathbf{r}}{\int \mathbf{E}^*(\mathbf{r}) \cdot \mathbf{D}(\mathbf{r}) d^3\mathbf{r}}. \quad (4)$$

The fill factor, which measures the amount of electric-field energy located inside the high-dielectric region, is shown in Table 1. Note that $f$ is large for the dielectric band but small for the air band, as we would expect from our qualitative analysis of the field patterns.

### TE Modes in Dielectric-Rod Array

The TE modes of the rod, for which there is only a small band gap, are displayed in Fig. 3. Like the TM modes, the TE modes would tend to be concentrated inside the dielectric regions to lower their frequency. However, there is no continuous pathway between the dielectric rods to contain the fields. Since the field lines must be continuous, they must penetrate the air regions. For this reason neither band is strongly concentrated in the dielectric region. Since the bands do not contrast strongly with each other, they do not have a large frequency splitting. Note that the vector nature of the electromagnetic field is crucial to understanding the band gap in this case. The scalar $\mathbf{D}$ field of the TM modes could easily be localized

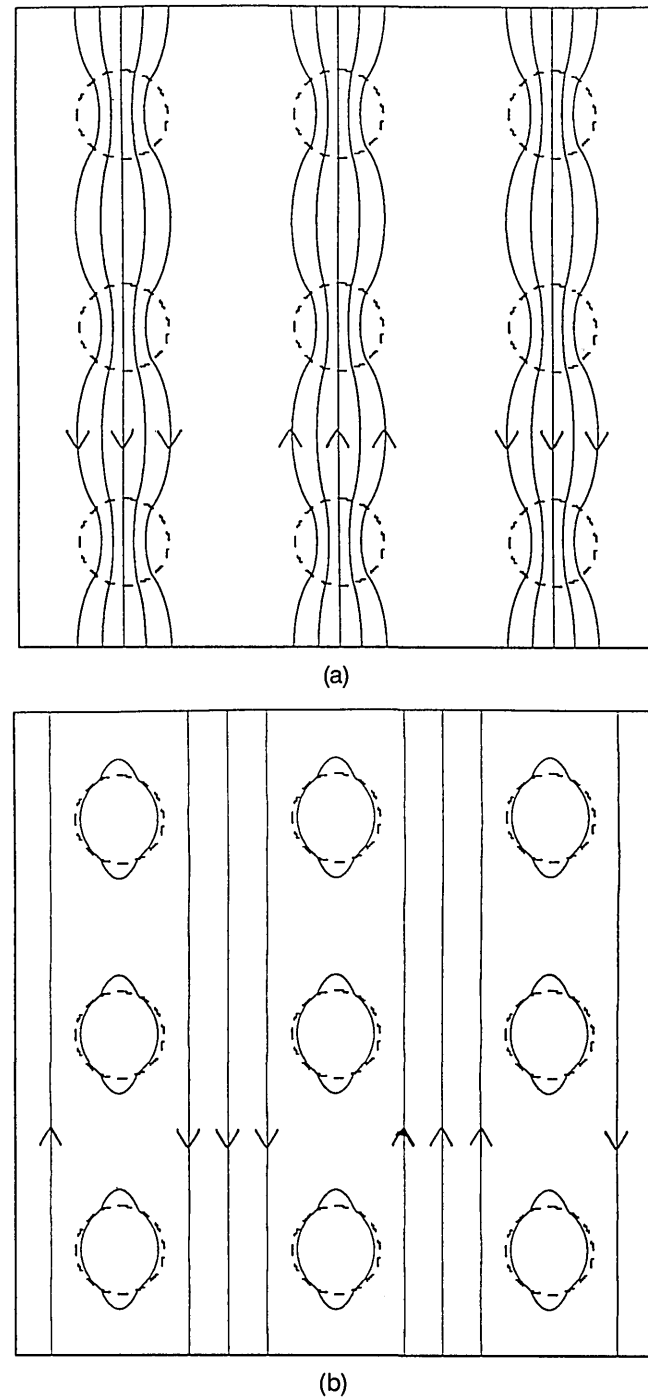


Fig. 3. Displacement fields of $X$-point TE states inside a square array of high-dielectric ($\epsilon = 8.9$) cylinders. TE modes have $\mathbf{D}$ in the plane $\mathbf{D}(\mathbf{r}) \cdot \hat{z} = 0$, and the figure shows the field lines of $\mathbf{D}$. Cylinders of high-dielectric material are enclosed by dotted circles, and the displacement field lines are shown as solid curves. (a) Dielectric-band state; (b) air-band state.

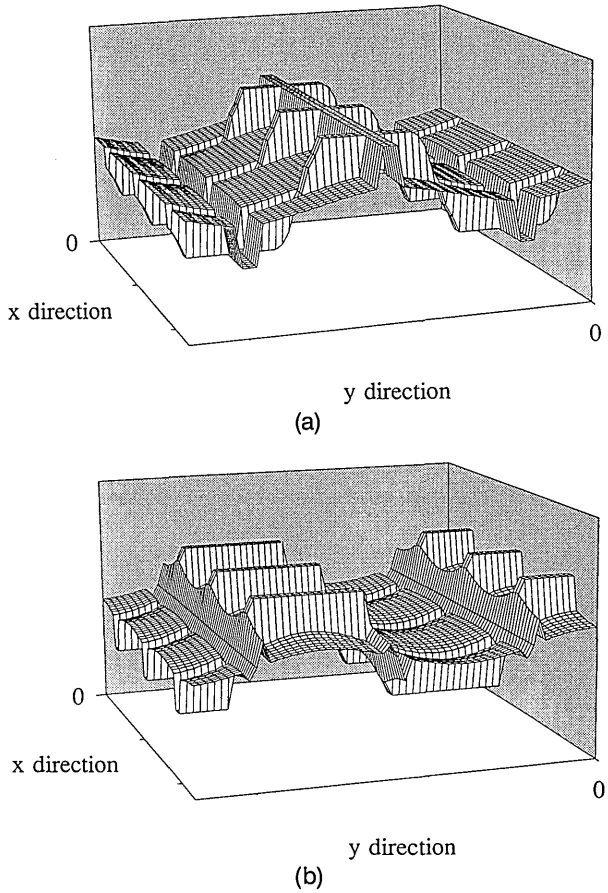


Fig. 4. Displacement fields of $X$-point TM states inside a square array of square holes in a high-dielectric ($\epsilon = 8.9$) material. TM modes have $\mathbf{D}$ normal to the plane, $\mathbf{D}(\mathbf{r}) = d(\mathbf{r})\hat{z}$. The height of the surface represents the size of the $z$ component of the displacement field. Positive peaks represent displacement fields pointing up the veins between square holes, and negative peaks show displacement fields pointing down the veins between square holes. (a) Dielectric-band state; (b) air-band state.

in the rods, but the continuous field lines of the TE modes must penetrate the air regions to connect neighboring rods.

The low fill factors for the modes shown in Fig. 3 confirm that both are concentrated in the air. It is confusing that the fields at the $M$ point show a large difference in fill factor but a small splitting. Fortunately, this is the only case that breaks the trend.

### TM Modes in Square-Hole Array

A study of the displacement field patterns in the square-hole array is equally revealing. Figure 4 shows the fields associated with the dielectric and the air bands of the TM mode for which there is only a small splitting. In this case both bands are contained predominantly within the dielectric regions. The fields of the dielectric band are confined to the square lattice of dielectric crosses, whereas the air band is contained in dielectric veins connecting the sites of the square lattice. The similarity of dielectric and air bands accounts for the lack of a TM gap. Again, this qualitative picture of the modes is confirmed by the fill factors shown in Table 2. Thus, in this case it was the lack of concentrated regions of dielectric material that prohibited us from forming a photonic band gap.

### TE Modes in Square-Hole Array

In Fig. 5 we see the displacement field lines for the TE modes of the square lattice, which do exhibit a photonic band gap. Unlike its counterpart in the rod lattice, the dielectric band of the square-hole array can extend its $\mathbf{D}$ field to neighboring lattice sites without ever leaving the dielectric regions. This situation is clearly shown in Fig. 5(a), which shows the field lines contained within the dielectric veins connecting the sites of the lattice. How-

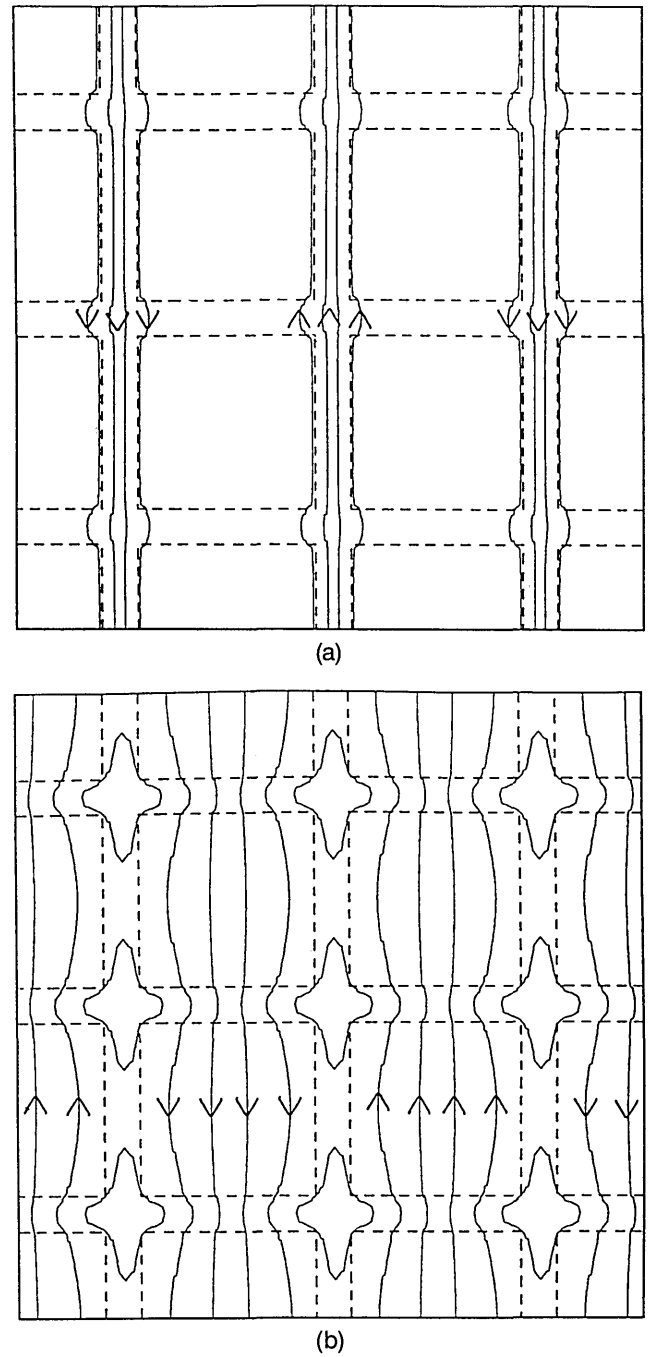


Fig. 5. Displacement fields of $X$-point TE states inside a square array of square holes in a high-dielectric ($\epsilon = 8.9$) constant. TE modes have $\mathbf{D}$ in the plane $\mathbf{D}(\mathbf{r}) \cdot \hat{z} = 0$, and the figure shows the field lines of $\mathbf{D}$. The regions of high-dielectric strength are enclosed by dotted curves, and the displacement field lines are shown as solid curves. (a) Dielectric-band state; (b) air-band state.

**Table 1. Fill Factors for the Lattice of Dielectric Rods**[a]

| Point | $f_{diel}$ | $f_{air}$ | $\Delta f$ | $\Delta\omega/\overline{\omega}$ |
|---|---|---|---|---|
| TM mode | | | | |
| *X* point | 83% | 32% | 51% | 46% |
| *M* point | 91% | 60% | 31% | 51% |
| TE mode | | | | |
| *X* point | 9% | 23% | −14% | 10% |
| *M* point | 60% | 10% | 50% | 9% |

[a] $f_{diel}$ and $f_{air}$ are the fill factors of the dielectric and air bands, respectively, and $\Delta f$ is their difference. $\Delta\omega/\overline{\omega}$ is the relative splitting of the band at that $k$ point, $(\omega_{diel} - \omega_{air})/[(\omega_{diel} + \omega_{air})/2]$. All data are presented for *M* and *X* points.

**Table 2. Fill Factors for the Lattice of Square Holes**[a]

| Point | $f_{diel}$ | $f_{air}$ | $\Delta f$ | $\Delta\omega/\overline{\omega}$ |
|---|---|---|---|---|
| TM mode | | | | |
| *X* point | 89% | 77% | 12% | 26% |
| *M* point | 92% | 86% | 6% | 16% |
| TE mode | | | | |
| *X* point | 83% | 14% | 69% | 54% |
| *M* point | 84% | 25% | 59% | 38% |

[a] $f_{diel}$ and $f_{air}$ are the fill factors of the dielectric and air bands, respectively, and $\Delta f$ is their difference. $\Delta\omega/\overline{\omega}$ is the relative splitting of the band at that **k** point, $(\omega_{diel} - \omega_{air})/[(\omega_{diel} + \omega_{air})/2]$. All data are presented for *M* and *X* points.

ever, the air band has a node passing through the veins and thus is forced into the air regions. This difference is confirmed in Table 2, which shows large fill factors for the dielectric band and small ones for the air bands. Because the first band has most of its character in the dielectric regions while the second has most of its character in the air, there is a large splitting between these bands. In this case it is the connectivity of the lattice that is crucial to yielding a photonic band gap.

Therefore our analysis of these two lattices has allowed us to uncover the features that are important for the development of a large two-dimensional photonic band gap. Concentrations of dielectric material were important to developing a photonic band gap for the TM polarization, while connectivity within the plane was important for band gaps in the TE polarization.

In closing we note that it is possible to obtain sufficient concentration and connectivity to produce a structure with a photonic band gap for both polarizations. At the dielectric contrast of GaAs ($\epsilon = 13$) a triangular lattice of air columns[12,13] exhibits such a gap. At a higher index contrast the square lattice of air columns[12] also possesses such a gap.

## ACKNOWLEDGMENTS

Partial support for this research was provided by U.S. Office of Naval Research contract N00014-86-K-0158. A. M. Rappe acknowledges the support of the Joint Services Electronics Program.

## REFERENCES

1. K. M. Ho, C. T. Chan, and C. M. Soukoulis, Phys. Rev. Lett. **65,** 3152 (1990).
2. E. Yablonovitch, T. J. Gmitter, and K. M. Leung, Phys. Rev. Lett. **67,** 2295 (1991).
3. R. D. Meade, K. D. Brommer, A. M. Rappe, J. D. Joannopoulos, Phys. Rev. B **44,** 13772 (1991).
4. E. Yablonovitch, T. J. Gmitter, R. D. Meade, K. D. Brommer, A. M. Rappe, and J. D. Joannopoulos, Phys. Rev. Lett. **67,** 3380 (1991).
5. R. D. Meade, K. D. Brommer, A. M. Rappe, J. D. Joannopoulos, Phys. Rev. B **44,** 10961 (1991).
6. W. Robertson, G. Arjavalingam, R. D. Meade, K. D. Brommer, A. M. Rappe, and J. D. Joannopoulos, "Observations of surface photons on periodic dielectric arrays," Opt. Lett. (to be published).
7. E. Yablonovitch, Phys. Rev. Lett. **58,** 2059 (1987).
8. J. Martorell and N. Lawandy, Phys. Rev. Lett. **65,** 1877 (1990).
9. E. Yablonovitch and T. J. Gmitter, Phys. Rev. Lett. **63,** 1950 (1989).
10. M. Plihal, A. Shambrook, A. A. Maradudin, and P. Sheng, Opt. Commun. **80,** 199 (1991).
11. S. L. McCall, P. M. Platzman, R. Dalichaouch, D. Smith, and S. Schultz, Phys. Rev. Lett. **67,** 2017 (1991).
12. P. Villeneuve and M. Piche, Phys. Rev. B **46,** 4969 (1992).
13. R. D. Meade, K. D. Brommer, A. M. Rappe, J. D. Joannopoulos, Phys. Rev. B **44,** 10961 (1991).
14. W. Robertson, G. Arjavalingam, R. D. Meade, K. D. Brommer, A. M. Rappe, and J. D. Joannopoulos, Phys. Rev. Lett. **68,** 2023 (1992).